Design of a microfluidic mixer channel

First steps into creating a fluorescent dye-based biosensor for mAb aggregate detection

São Pedro, Mariana N.; Santos, Mafalda S.; Eppink, Michel H.M.; Ottens, Marcel

DOI
10.1002/biot.202200332

Publication date
2022

Document Version
Final published version

Published in
Biotechnology Journal

Received: 27 June 2022 | Revised: 29 August 2022 | Accepted: 6 September 2022

DOI: 10.1002/biot.202200332

Biotechnology Journal

RAPID COMMUNICATION

Design of a microfluidic mixer channel: First steps into creating a fluorescent dye-based biosensor for mAb aggregate detection

Mariana N. São Pedro[1] | Mafalda S. Santos[1] | Michel H. M. Eppink[2,3] | Marcel Ottens[1]

[1]Department of Biotechnology, Delft University of Technology, Delft, the Netherlands

[2]Byondis B.V., Nijmegen, the Netherlands

[3]Bioprocessing Engineering, Wageningen University, Wageningen, the Netherlands

Correspondence
Marcel Ottens, Department of Biotechnology, Delft University of Technology, Van der Maasweg 9, Delft, 2629 HZ, the Netherlands.
Email: m.ottens@tudelft.nl

Abstract

A major challenge in the transition to continuous biomanufacturing is the lack of process analytical technology (PAT) tools which are able to collect real-time information on the process and elicit a response to facilitate control. One of the critical quality attributes (CQAs) of interest during monoclonal antibodies production is aggregate formation. The development of a real-time PAT tool to monitor aggregate formation is then crucial to have immediate feedback and process control. Miniaturized sensors placed after each unit operation can be a powerful solution to speed up an analytical measurement due to their characteristic short reaction time. In this work, a micromixer structure capable of mixing two streams is presented, to be employed in the detection of mAb aggregates using fluorescent dyes. Computational fluid dynamics (CFD) simulations were used to compare the mixing performance of a series of the proposed designs. A final design of a zigzag microchannel with 45° angle was reached and this structure was subsequently fabricated and experimentally validated with colour dyes and, later, with a FITC-IgG molecule. The designed zigzag micromixer presents a mixing index of around 90%, obtained in less than 30 seconds. Therefore, a micromixer channel capable of a fast and efficient mixing is hereby demonstrated, to be used as a real-time PAT tool for a fluorescence based detection of protein aggregation.

KEYWORDS

computational fluid dynamics, continuous biomanufacturing, microfluidics, Process Analytical Technology (PAT), protein aggregation

1 | INTRODUCTION

In recent years, the biopharmaceutical industry has demonstrated a growing interest in implementing continuous biomanufacturing, especially for the production of monoclonal antibodies (mAbs).[1,2] A major challenge which still needs to be tackled to implement continuous bioprocessing is the development of process analytical technologies (PAT).[3] By creating at-line sensors which can provide a real-time measurement of product critical quality attributes (CQAs), PAT will provide control within a continuous process and elicit a timely response.[1] Product aggregation, a poorly understood phenomenon, is considered a critical CQA in the manufacturing of mAbs. Several environmental and process factors are known to induce aggregation, such as the low pH employed during the viral inactivation step[4] or the shear stress

Abbreviations: 2D, two-dimensional; 3D, three-dimensional; CFD, Computational Fluid Dynamic; CQA, Critical Quality Attribute; DoL, Degree of labeling; HMW, High Molecular Weight; mAb, Monoclonal Antibody; MI, Mixing Index; PAT, Process Analytical Technology; PDMS, Polydimethylsiloxane; ROI, Region Of Interest.

induced from pumps.[5] Therefore, the formation of high molecular weight (HMW) species is unavoidable and the measurement of this CQA is crucial to elicit a real-time control of the aggregation inducing factors.

Several analytical techniques are available for the study and characterization of protein aggregates such as dynamic light scattering or Raman spectroscopy.[6] However, these techniques are characterized by lengthy analysis times.[1,7] Fluorescent dyes, such as SYPRO Orange and 4-4-bis-1-phenylamino-8-naphthalene sulfonate (Bis-ANS), are sensitive to the hydrophobicity of the surrounding environment. Since aggregate formation generates hydrophobic unfolded protein structures, these fluorescent tags can be used to rapidly detect this phenomenon.[8–10] The dye's fluorescence intensity significantly intensifies when in the contact to the hydrophobic patches, providing a straightforward and instantaneous measurement.[3] Fluorescent dyes can be used as a stand-alone characterization method[10,11] or in combination with other analytical techniques[12] for a rapid measurement, demonstrating the great potential of applying it in a PAT tool. Miniaturized sensors are considered to be a possible solution to speed up the analytical measurements of CQAs due to the inherent short operation time.[3] Additionally, microfluidic chips are characterized by the use of minimal amounts of samples (in the µL or nL-scale) and, depending on the material, being relatively affordable and easily fabricated.[13] Therefore, by combining the advantages of fluorescence-based methods with the miniaturization of analytical technologies, a miniaturized tool for real-time detection of mAb aggregates can be achieved, with the microfluidic device working at-line.

When designing a fluorescent dye-based miniaturized sensor, a major problem arises: the fluorescent dye stream needs to be fast and efficiently mixed with the mAb sample stream. The small characteristic dimensions of such sensors combined with the low fluid velocities typically used leads to low Reynolds numbers (Re) and, consequently, to the presence of a laminar flow regime.[14] In such regimes, fluids flow in parallel layers, with no disruption, and mixing is dominated by molecular diffusion, an inherently slow process. Therefore, to preserve the small dimensions of microfluidic devices and to increase their throughput, it is essential to increase the contact area of the fluidic layers and induce chaotic advection to obtain the necessary fast and efficient mixing.[15,16] Several strategies have been used to enhance the mixing efficiency in laminar flow regimes, including the passive mixing methods.[16,17] Passive mixing is accomplished by altering the structure or configuration of microfluidic channels,[3] such as using distinct zigzag angles,[18] serpentine configurations[14,19] or the incorporation of obstructions in the middle of the channel.[20] The simple design, fabrication and operation of the microfluidic chips employing passive methods[14] make them the preferred approach. Even though many passive micromixers have been reported in literature, the mixing performance of the devices was determined under dissimilar conditions from those required for a fluorescent dye-based sensor. A screening of possible geometries and, subsequently, its mixing efficiency must then be performed, taking into account the characteristics of the fluorescent dye and the mAb streams.

In the present study, the development of a micromixer channel to mix a fluorescent dye with a mAb stream is demonstrated, to potentially be used as real-time aggregate detection tool. First, the design of a passive mixing channel employing different geometries to induce the mixing of two streams is discussed. To study the mixing efficiency of each proposed design, a computational fluid dynamic (CFD) model was developed. From all the assessed geometric configurations, a zigzag channel with a 45° angle, providing a residence time of 30 s, showed the highest mixing efficiency. The proposed zigzag mixing channel is experimentally validated, first, resorting to color dyes, and then to a fluorescent tagged IgG molecule (FITC-IgG).

2 | MATERIALS AND METHODS

Poly(dimethylsiloxane) (PDMS) was purchased as a Sylgard 184 elastomer kit (Dow Corning, Midland, MI). Standard food colorant dyes (blue and yellow dyes) were obtained from Jo-La (Bharco Foods B.V., Diemen, The Netherlands). IgG from human serum conjugated with the fluorescent dye FITC was acquired from Sigma-Aldrich (Sigma-Aldrich Chemie BV, Zwijndrecht, The Netherlands). Sodium phosphate monobasic dehydrate, di-sodium hydrogen phosphate and sodium chloride were purchased from Sigma-Aldrich, Merck (Merck KGaA, Darmstadt, Germany) and VWR Chemicals (VWR International, Radnor, PA, United States), respectively.

2.1 | Microfluidic structure design

Four micromixers with different geometries were designed in AUTOCAD® (Version 23.0): a zigzag, a curved serpentine, a square serpentine and a straight T-mixer channel (Figure 1). All designed micromixers display two inlets from which the working fluids are supplied separately. The two inlets are connected by a T-joint that leads the fluids to the mixing channel, which, at the end, is also connected to a straight channel, the outlet channel, through which the mixed fluids exit the device. Additionally, geometric variations of the zigzag micromixer were explored, varying the zigzag angle, φ, at 30°, 45°, 60° and 82°.

2.2 | Numerical simulations

2.2.1 | Numerical model

Commercial CFD software COMSOL Multiphysics (Version 5.6) was employed to analyze the flow patterns and mixing behavior inside the designed micromixers. Two interfaces, *Laminar Flow* and *Transport of Diluted Species*, were utilized, with the multiphysics node *Reacting Flow, Diluted Species* applied to couple the interfaces (Figure 2). The Laminar Flow interface was used to compute the velocity and pressure fields by solving the Navier-Stokes and continuity equations. The fluid was assumed to be Newtonian and the flow incompressible, laminar and at

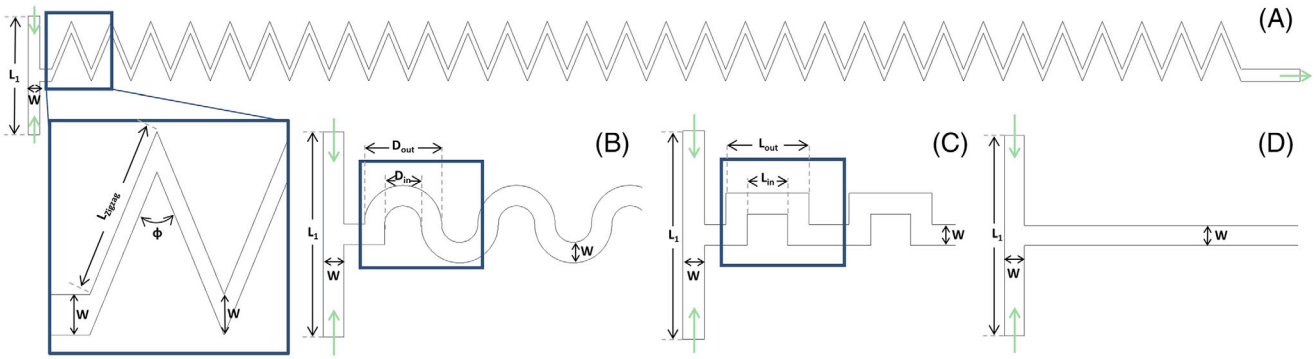

FIGURE 1 Schematic representation of the designed passive mixing structures, each with 30 mixing units and a total length of the mixing channel of around 26.25 mm: (A) Zigzag channel, with $\varphi = 45°$; (B) Curved serpentine; (C) Square serpentine; and (D) T-mixer. The description and value of each parameter can be found in Table 1. In blue, the mixing unit from each designed structure is highlighted. The green arrows indicate the flow of both liquids entering in the two inlets and the resulting mixed liquid exiting in the outlet.

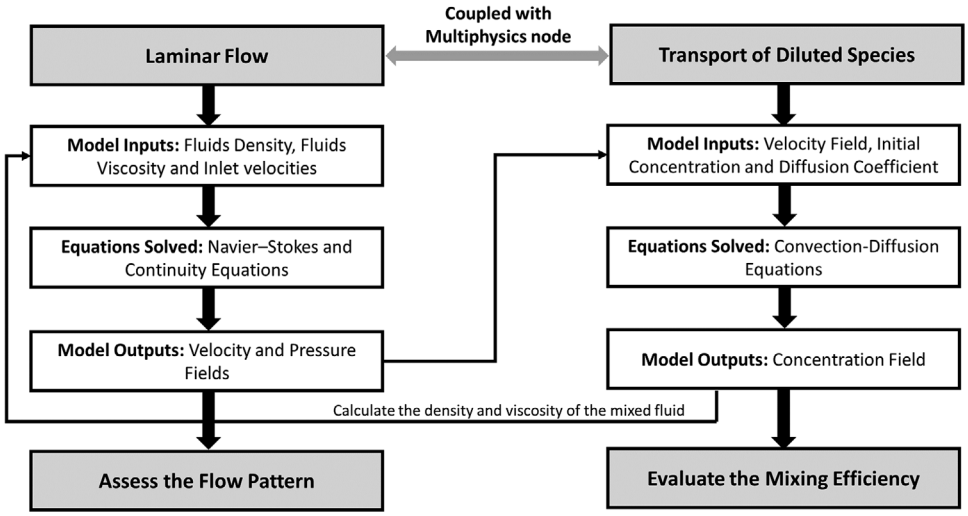

FIGURE 2 Schematic representation of the numerical model developed to analyze the flow pattern and mixing efficiency of the designed micromixers, with the interfaces adopted and their inputs and outputs.

steady-state, and can be expressed as:

$$\rho (v \cdot \nabla) v = \nabla \cdot \left[-pI + \mu \left(\nabla v + (\nabla v)^T \right) \right] \quad (1)$$

$$\rho \nabla \cdot (v) = 0 \quad (2)$$

where ρ is the density, v is the velocity, p is the pressure, I is the identity matrix and μ is the dynamic viscosity of the fluid. The velocity field obtained was then used to calculate the concentration field using the *Transport of Diluted Species* interface, which solved the convention-diffusion equation:

$$\nabla \cdot (D_c \cdot \nabla c) = v \cdot \nabla c \quad (3)$$

where D_c is the diffusion coefficient and c is the concentration. To solve Equations (1), (2), and (3), the following boundary conditions were set: 1) the velocity and mass flux are zero at the walls of the channel; 2) the fluid velocity and concentration at the inlets are defined; and 3) the static pressure at the outlet was set to zero. Since the Laminar Flow interface is used to simulate single-phase fluids, a single input of density and of viscosity had to be used. However, both fluids used in the study had dissimilar values of density and viscosity. Thus, density and viscosity of the mixed fluid were defined, at each point of the channel, as a function of the fraction of fluid supplied at inlet 1 present at that point ($f_{inlet1,i}$):

$$\rho_{fluid} = \rho_{inlet1} \cdot f_{inlet1,i} + \rho_{inlet2} \cdot \left(1 - f_{inlet1,i}\right) \quad (4)$$

$$\mu_{fluid} = \mu_{inlet1} \cdot f_{inlet1,i} + \mu_{inlet2} \cdot \left(1 - f_{inlet1,i}\right) \quad (5)$$

The multiphysics node *Reacting Flow, Diluted Species* was then used to couple the concentration field, obtained from the *Transport of Diluted Species* interface, as an input to the *Laminar Flow* interface, to compute the value of $f_{inlet1,i}$.

Since COMSOL Multiphysics is based on the finite element method (FEM), the designed structures needed to be divided into a mesh comprised of a number of small units of simpler shapes. The structures were then discretized using quadrilateral and triangular elements. Grid independence tests were carried out with different numbers of mesh elements. For the initial studies into the different geometries, to save computational time and power, a mesh of 1.22×10^5, 2.73×10^5, 3.31×10^5 and 2.53×10^5 elements were selected for the T-Mixer, Square Serpentine, Curved Serpentine and Zigzag Channel, respectively. For the angle variation studies in the zigzag micromixer, a mesh of 1.68×10^5, 2.50×10^5 and 3.18×10^5 elements for φ of 30°, 45° and 60°, were chosen, respectively.

The mixing index (MI) of each proposed micromixer was evaluated based on the standard deviation of the concentration at a given cross section[21]:

$$MI = 100\% - \frac{\sigma}{\sigma_{\max}} = \frac{\sqrt{\sum_{i=1}^{N}(c_i - c_m)^2}}{\sqrt{\sum_{i=1}^{N}(c_0 - c_m)^2}} \quad (6)$$

where σ is the standard deviation of the point concentration to the optimal concentration at a given cross section, σ_{max} is the standard deviation of the concentration at a completely unmixed section, c_i is the concentration at a sample point i, c_m is the optimal concentration (50 g L^{-1}), c_0 is the point concentration at a completely unmixed cross section (0 or 100 g L^{-1}) and N is the total number of sampling points. MI will thus vary between 0, totally unmixed state, and 100%, completely mixed state.

2.2.2 | Model Implementation

Firstly, with the proposed numerical model, all the designed micromixers were tested for the mixing efficiency, using two-dimensional (2D) numerical simulations. An aqueous mAb solution and a highly diluted fluorescent dye solution were used as the working fluids for the numerical analysis. A density of 998 kg m^{-3} and a viscosity of 1.01×10^{-3} Pa · s were applied for the fluorescent dye solution.[22] For the mAb solution, a density of 1037 kg m^{-3},[23] a viscosity of 6×10^{-3} Pa · s,[24] a diffusion coefficient of 1.5×10^{-11} m^2 s^{-1}[24] and a concentration of 100 g L^{-1} were assumed. Since no mAb is present in the fluorescent dye stream, its concentration was defined at zero. Different ranges of both inlet velocities were employed, ranging from 1×10^{-5} to 1×10^{-2} m s^{-1}.

The numerical model was also used for three-dimensional (3D) numerical simulation for the zigzag structure with $\varphi = 45°$. The height of the microchannel was defined at 100 µm. The previously described proprieties for the mAb and fluorescent dye solutions were used as working fluids. Both inlet velocities were set to 1×10^{-3} m s^{-1} and a mesh with 3.28×10^6 elements was selected to perform this study.

Additionally, a parametric study was performed for the zigzag structure with $\varphi = 45°$, using multiphysics study type *Parametric Sweep* and *All combinations* as the type of sweep. The 3D numerical model was used, with the same defined variables, except for the viscosity and density of the mAb solution. The set of mAb solutions viscosities used were: 2×10^{-3}, 4×10^{-3}, 6×10^{-3}, and 8×10^{-3} Pa · s. For the diffusion coefficient, the values studied were: 1×10^{-11}, 5×10^{-11}, 7.5×10^{-11}, and 10.5×10^{-11} m^2 s^{-1}. Since *All combinations* was selected as the type of sweep, the model was solved for all combinations of viscosity and diffusion coefficient values, with a mesh of 8.50×10^5 elements.

2.3 | Experimental validation

2.3.1 | Structure fabrication

Two microfluidic devices were fabricated: a T-mixer straight microchannel (100 µm high × 100 µm wide× 26.3 mm long) and a zigzag microchannel (100 µm high x 100 µm wide x 17.2 mm long) with two inlets and one outlet (each 100 µm wide). The designed mold was ordered from INESC Microsystems and Nanotechnologies (Lisbon, Portugal) and the structures were fabricated using a 7:1 mixture of PDMS and curing agent. After being degassed, the mixture is poured onto the mold and baked at 80°C for 45 min. After the PDMS is cured, the chip is removed from the mold and the inlets and outlet are punched. Finally, the PDMS chip is bonded to a glass substrate and sealed with a 20:1 mixture of PDMS to curing agent.

2.3.2 | Color dyes and FITC-IgG

A syringe pump KD Scientific 200 (KD Scientific Inc, Holliston, MA) was used to pump in two different streams into the microfluidic structure, with a flow rate of 1 µL min^{-1}. Firstly, the micromixer was validated using two color dyes (blue and yellow), and then with a fluorescent tagged IgG molecule (FITC-IgG) and a buffer solution (50 mM sodium phosphate buffer, 150 mM sodium chloride, pH 7.2, prepared in Milli Q water). FITC-IgG was diluted to a concentration of 5 mg mL^{-1} with the same buffer. An inverted fluorescence microscope (Leica DMI 5000 M, 10× objective, Leica Microsystems BV, The Netherlands) and a digital camera (Leica DFC300 FX, Leica Microsystems BV, The Netherlands) were used for the acquisition of bright field and fluorescence images. The fluorescence images of FITC-IgG were obtained by using a Leica L5 filter cube (excitation: BP 460–488 nm; emission: 502–547 LP nm). All the acquired images were processed and analyzed using Image J.

The mixing efficiency was then analyzed based on the color RGB (red, green and blue) components of the images obtained. For the color dye validation, the image was split and each generated image measured according to a grayscale (the value of each pixel is a single sample representing the amount of light, varying from 0, completely black, to 255, completely white). A circular region of interest (ROI), with a radius of 15 µm, was selected after each mixing unit, in the blue stream, and the color intensity measured. To quantify the color yellow, the green and red measurements were added, and the color blue corresponds to the blue measurement. Considering the blue color, the MI can then be calculated:

$$MI = 100\% - \left(\%B_{left} - D_{mixed}\right) \quad (7)$$

where $\%B_{left}$ is the amount of blue present in the ROI and D_{mixed} is the difference of blue to yellow in a 1:1 mixture, which was determined to be 0. Therefore, Equation (7) can be rewritten:

$$MI = 100\% - \left(\frac{B_{image} - Y_{image}}{B_{unmixed}} \times 100\%\right) \quad (8)$$

where B_{image} is the amount of blue measured in the ROI, Y_{image} is the amount of yellow measured in the ROI and $B_{unmixed}$ is the amount of blue in an unmixed state, measured in the beginning of the channel. For the FITC-IgG validation, a similar approach was followed for the selection of the ROI. However, since only the green color had to be taken into account, the MI was calculated according to:

$$MI = 100\% \times \frac{G_{buffer}}{G_{mixed}} \quad (9)$$

where G_{buffer} is the amount of green in the ROI of the buffer stream and G_{mixed} is the amount of green in the ROI in a 1:1 mixture of fluorescent dye to buffer.

TABLE 1 Description and the value of the several geometric parameters used in the designed structures (identified in Figure 1).

Parameter	Description	Measure
L_1	Transverse length of the T-junction	1000 μm
W	Width of the main channel	100 μm
L_{Zigzag}	Length of the zigzag channel diagonal	440 μm
$\Phi^{a)}$	Angle of the zigzag channel	45°
D_{in}	Diameter of the inner walls of the curved serpentine	180 μm
D_{out}	Diameter of the outer walls of the curved serpentine	380 μm
L_{in}	Length of the inner walls of the square serpentine	190 μm
L_{out}	Length of the outer walls of the square serpentine	390 μm

The value of the parameter was kept constant in all designed structures, except for φ which was also varied at 82°, 60°, and 30°.

3 | RESULTS AND DISCUSSION

3.1 | Design of the microfluidic channel

When developing a real-time miniaturized PAT tool for aggregate detection, critical criteria should be fulfilled by the designed structure for a straightforward implementation in a continuous process: 1) the micromixer must not alter the amount of aggregates present in the initial sample; 2) the designed structure should provide high mixing efficiency, with a settled minimum efficiency of 90%; 3) to facilitate process control, the microfluidic device has to provide a fast measurement (within a time range of seconds to a few minutes). Additionally, it is also beneficial that the designed micromixer is simple and easily fabricated, as well as presenting reduced footprint, to allow a smoother implementation. Therefore, considering the imposed criteria, four different microchannel geometries were assessed: a straight T-mixer channel, a square serpentine, a curved serpentine and a zigzag channel (Figure 1). The mixing length of each of the proposed designs was fixed at around 27 mm, with a total of 30 mixing units. The dimensions of each mixing unit were defined in order to meet this total mixing length (Table 1) to guarantee that the mixing is dependent not only on the length but also on the flow patterns induced by the different geometries. Furthermore, the T-mixer was also designed as a control to determine to what extent mixing was dependent on the mixing length.

Firstly, to perform a comparative analysis of each microchannel geometry, and subsequently, its mixing efficiency, a CFD model was developed. Resorting to COMSOL Multiphysics, two interfaces, Laminar Flow and Transport of Diluted Species, were employed, with the multiphysics node Reacting Flow, Diluted Species coupling the interfaces (Figure 2). These numerical simulations were conducted under conditions that mimic those found in practice for the detection of mAb aggregates. Since the fluorescent dye solutions commonly used to analyze aggregates are highly diluted, the proprieties of water at 20°C were used.[22] The mAb solution was considered to have the composition commonly found in the formulation step, high protein and low excipients concentrations, with a mAb concentration of 100 g L^{-1} being employed. Then, the properties of the mAb solution (diffusion coefficient, viscosity and density) were based on this concentration[23,24] chosen to test the designed structures under the most unfavorable conditions.

To compare the mixing performance of the proposed designs, the MI at the end of each mixing channel was calculated (Equation (6)) and is shown in Figure 3A. A wide range of inlet velocities, from 1×10^{-5} to 1×10^{-2} m s^{-1}, was used to assess its impact on the mixing efficiency, resulting in a Reynolds number (*Re*) ranging from 3×10^{-4} to 0.3. At low velocities (and subsequently low *Re*), viscous forces are dominant. Consequently, the strength of the secondary flows is not sufficient to significantly disturb the parallel fluid layers and mixing is solely dominated by molecular diffusion. Thus, the high MI observed for lower velocities across all structures is due to longer residence times and larger contact areas. As the inlet velocities and *Re* increases, a decrease in the MI is observed due to shorter retention times and, thus, less efficient molecular diffusion. These parallel fluid layers are represented in the T-mixer velocity arrow plot obtained from COMSOL (Figure 3B), where it is possible to observe the fluid flowing in parallel without any path crossing. By analyzing the remaining arrow plots (Figure 3C-E) at the velocity of 1×10^{-3} m s^{-1}, the designed structures presented regions where the parallel layers were disturbed and the streams path crossed. For example, the zigzag structure (Figure 3E) showed a disturbance area next to the corner of the structure. Likewise, the square serpentine structure (Figure 3C) exhibited several disturbance regions near the turns. These path crossing areas were then responsible for increasing the MI since they increase the contact area between the fluids. Because these areas were more pronounced in the square

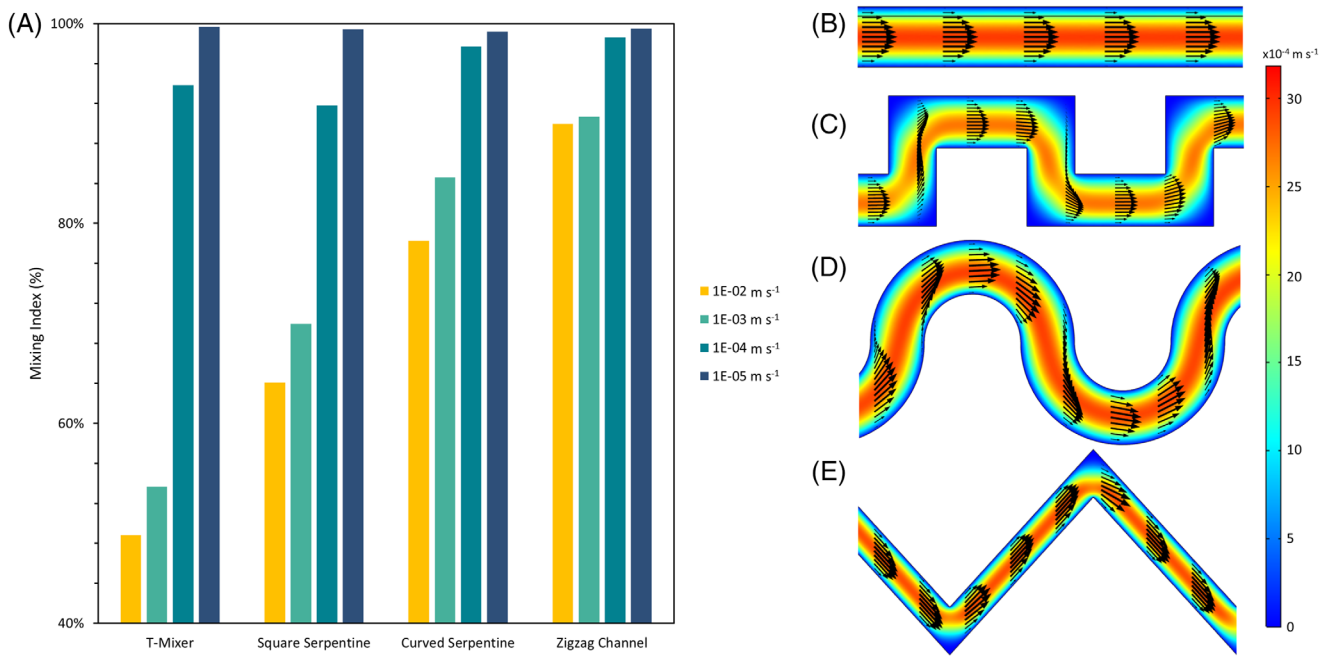

FIGURE 3 (A) Mixing index of each of the passive micromixers, with 30 mixing units, at the exit of the channel, with different velocities defined at both inlets: 1×10^{-2}, 1×10^{-3}, 1×10^{-4}, and 1×10^{-5} m s^{-1}, with a Reynolds number varying from 3×10^{-4} to 0.3. Velocity arrow plots obtained from COMSOL, in the last mixing unit, at $v = 1 \times 10^{-3}$ m s^{-1}: (B) T-mixer; (C) Square Serpentine; (D) Curved Serpentine; and (E) Zigzag channel ($\varphi = 82°$).

serpentine, followed by the zigzag and lastly by the curved serpentine (Figure 3D), it was expected the mixing efficiency would follow the same order. However, the square serpentine showed a lower MI. The presence of more predominant void areas (in blue) is observed, where the fluid is not able to reach. These void areas might counterbalance the path crossing phenomenon, especially at higher velocities. The curved serpentine, where the void areas are almost negligible, presents a higher MI than the square serpentine. Thus, the mixing in the designed structures will depend on the balance of these two phenomena, the presence of path crossing and void areas in the channel. The zigzag structure was more efficient because the presence of void volumes was more favorably counterbalanced by the presence of path crossing regions, having a MI of at least 90% at all tested velocities. Therefore, this zigzag geometry will then be explored to further increase its mixing efficiency.

To further manipulate the two aforementioned mixing phenomena and enhance the MI, variations in the zigzag angle were performed, ranging from the initial 82° to 30°. From Figure 4E, by decreasing the angle to 45°, a higher MI is obtained compared to the initial 82°, especially at higher velocities. The decrease in the path crossing area is then more favorable to induce the mixing, even though the void area of the corner increases (Figure 4A,C,D). When decreasing the zigzag angle to 30° angle, the MI slightly drops. The increase on the void area is no longer counterbalanced by the increase in the flow disturbance area (Figure 4B). When comparing the MI reached with 45° and 60° angles, only a 1% difference is encountered at all velocities tested. Although the 60° angle presents a slightly higher MI, the 45° angle presents a smaller footprint structure, an important imposed design criteria. Hence, the zigzag channel with a 45° angle will be the design selected to create this fluorescent dye-based PAT tool.

3.2 | 3D Simulations

The CFD model was firstly developed and implemented in 2D since it demands less computational resources and time than its 3D counterpart. Thus, the 2D simulations were used as a screening tool into mixing efficiency of the different geometries, while the more physically accurate 3D simulations were used to confirm the previously obtained results. A velocity of 1×10^{-3} m s^{-1} was used since fluid velocities of this order of magnitude are commonly used in microfluidic devices.[16,17] The results obtained for the MI in the 3D simulations are present in Figure 5A(). At the exit of the structure, a slightly higher MI of approximately 98% was obtained, when compared to 97% of the 2D simulations. This difference might be due to the extra dimension of the height of the channel taken into account in the 3D simulations. Thus, the path crossing of both fluids also occurs vertically, providing better and faster mixing. Additionally, in the 3D simulations, the MI of 98% is already achieved after the 5th mixing unit. Then, based on the 3D simulations, the final zigzag structure can have less than 30 mixing units. Nevertheless, the MI obtained is solely based on CFD simulations. Thus, these results have to experimentally validated and the selection of the optimal number of mixing units should be based on the latter.

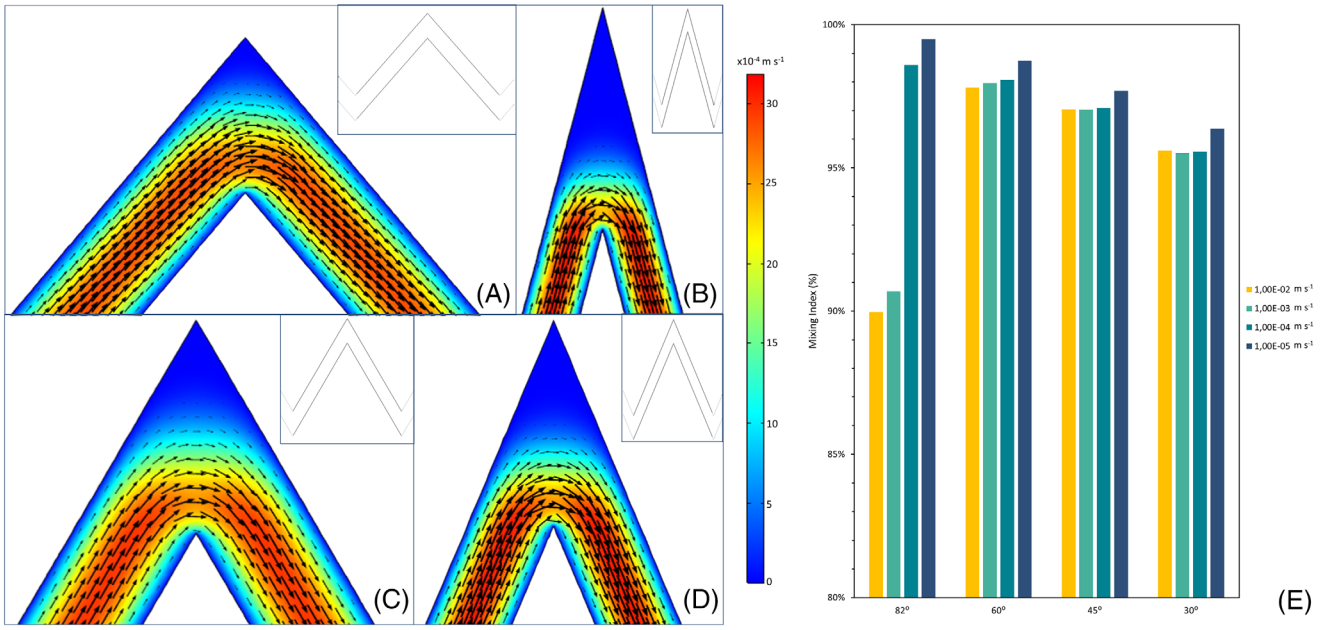

FIGURE 4 Geometric variation of the angle, φ, and the corresponding velocity arrow plots obtained from COMSOL, in the last mixing unit, at $v = 1 \times 10^{-3}$ m s^{-1}: (A) 82°; (B) 30°; (C) 60°; and (D) 45°. (E) Mixing index of each of the geometric variations, with 30 mixing units, at the exit of the channel, with different velocities defined at both inlets: 1×10^{-2}, 1×10^{-3}, 1×10^{-4}, and 1×10^{-5} m s^{-1}.

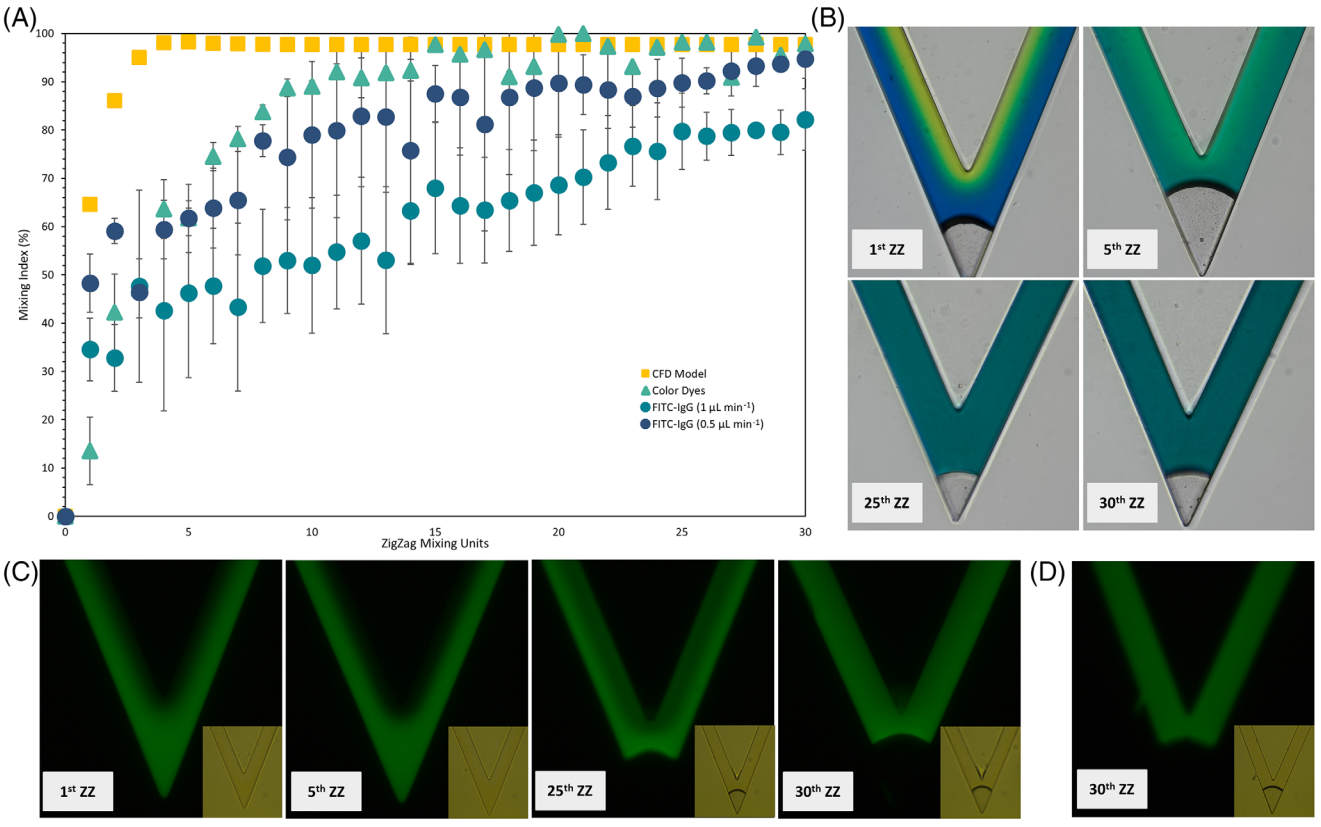

FIGURE 5 (A) Comparison of the mixing index obtained from the 3D CFD model ( ), the experimental validation using color dyes ( ), and using the FITC-IgG molecule, at a flow rate of 1 µL*min*$^{-1}$ and 0.5 µL *min*$^{-1}$ (and , respectively). All experimentally measured MI values are the average of two experiments and the error bars represent the standard deviation (± SD). (B) Bright field microscope images from the experimental validation of the zigzag channel using color dyes, from the 1st, 5th, 25th, and 30th zigzag unit, acquired with the objective 10x. (C) Fluorescence microscope images from the experimental validation of the zigzag channel using FITC-IgG, at a flow rate of 1 µL *min*$^{-1}$, from the 1st, 5th, 25th, and 30th zigzag unit, acquired with the objective 10x, exposure time of 50 ms and gain 0. (D) Fluorescence microscope images from the experimental validation of the zigzag channel using FITC-IgG, at a flow rate of 0.5 µL *min*$^{-1}$, from the 30th zigzag unit, acquired with identical conditions to (C).

Other design requirements were also evaluated with the 3D model. The shear rate which the mAb molecule would be subjected to in the microchannel was addressed since one of the design requirements is that the structure itself must not affect the amount of aggregates. According to the 3D simulations, the shear rate which the fluid is exposed to was below $1.76 \times 10^3\ s^{-1}$. Bee et al.[25] exposed highly concentrated mAb solutions to shear rates between 2×10^4 and $2.5 \times 10^5\ s^{-1}$ for 5 minutes. No aggregation in the stressed samples were detected by several analytical techniques (dynamic light scattering, analytical ultracentrifugation, etc.). Hence, the structure, which calculated a lower shear rate, is not expected to change the sample's level of aggregation.

Pressure drop, the difference of pressure in the beginning and in the end of the mixing channel, was also evaluated within the microchannel to assess the integrity of the device. A pressure drop of $4.5 \times 10^3\ Pa$ across the structure was calculated. Therefore, the pressure drop was sufficiently small for cheap fabrication materials, like PDMS, to be used without jeopardizing the integrity of the structure during its operation.

The mixing length (L_{mix}) of 26.25 mm was also determined based on the following equation:

$$L_{mix} = 2 \times N_{MU} \times L_{zigzag} \quad (10)$$

where N_{MU} is the number of mixing units, 30, and L_{zigzag} is the length of the zigzag channel diagonally (Table 1). Knowing the mixing length, the mixing time can be calculated, taking also into account the length of the T-junction and velocity used. A mixing time (t) of 27.5 seconds was achieved for the designed structure, showing that it is not only able to provide a high mixing efficiency, but also a fast measurement in the time range of seconds.

Lastly, one imposed requirement was a reduced footprint of the micromixer, which was determined using the mixing length and amplitude of the zigzag angle. A 10.75 mm^2 footprint was calculated, satisfactory for a passive mixer, which normally ranges from a few mm^2 to cm^2.[26]

3.3 | Parametric studies

The excipients typically found in mAb formulations may impact the fluid properties. Additionally, the micromixer can be used in other steps of the mAb manufacturing process, where the mAb solution properties will differ from those previously chosen in the CFD simulations. Plus, different mAbs typically present quite disparate transport properties.[24] A robust structure which can provide rapid and efficient mixing over a broad range of mAb solutions conditions is then crucial. Therefore, to take into consideration the impact of different excipients and solution properties, a parametric study for the MI was performed to cover a wide range of conditions. The viscosity was varied between 2×10^{-3} and 8×10^{-3} Pa · s and the diffusion coefficient between 1×10^{-11} and $10.5 \times 10^{-11}\ m^2\ s^{-1}$, values found in literature.[24,27,28] The MI obtained for all the assessed values, viscosity and diffusion coefficient, can be found in Table 2. The mixing efficiency is mainly dependent on the viscosity: solutions with lower viscosities reached higher MI values. At higher viscosities, some parts of the structure were unavailable and, therefore, mixing was hindered in those regions. Nevertheless, only slight differences in the MI were reached, with values ranging from 97% to almost 100% for all combinations of viscosity and diffusion coefficient tested. The robustness of the mixing efficiency of the proposed structure is then demonstrated. The developed PAT tool is able to be used as an universal method to detect the formation of aggregates through all the various steps in the manufacturing process.

TABLE 2 Mixing index obtained in the parametric study for the zigzag structure with $\varphi = 45°$, varying the diffusion coefficient, D_c, between 1×10^{-11} and $10.5 \times 10^{-11}\ m^2 s^{-1}$, and the viscosity, μ, between 2×10^3 and $8 \times 10^3\ Pa\ s$, of the mAb stream properties in the 3D numerical model.

	$D_c\ (m^2 s^{-1})$			
$\mu(Pa\ s)$	1×10^{-11}	5×10^{-11}	7.5×10^{-11}	10.5×10^{-11}
2×10^3	99.94%	99.89%	99.87%	99.86%
4×10^3	98.57%	98.61%	98.63%	98.65%
6×10^3	97.83%	97.87%	97.89%	97.91%
8×10^3	97.40%	97.40%	97.42%	97.45%

3.4 | Experimental validation

With the final design for the micromixer achieved, a zigzag channel with a 45° angle and 98% of mixing efficiency, the next step was to experimentally validate the calculated MI. Firstly, the zigzag and a T-mixer channel (with an identical mixing length) were fabricated and, resorting to standard color dyes, the MI was experimentally validated. Blue and yellow dyes were used and the formation of green throughout the channel was analyzed, with the results obtained present in Figure 5A(). When analysing Figure 5B, it is possible to observe the formation of the color green throughout the mixing channel, with a perfect mixing of blue and yellow being achieved by the 25th mixing unit. Even though a MI of 98% is still reached by the end of the channel, the mixing is considerably slower. The high MI is not achieved by the 5th mixing unit (Figure 5B) as the CFD model predicted, but on the 15th mixing unit. The color dyes possess different physical proprieties than the highly concentrated mAb solution used in the 3D simulations, explaining the slower mixing. Nevertheless, it still provides satisfying mixing and indicates that the zigzag channel is able to efficiently mix two streams. Furthermore, the T-mixer channel was also validated and was able to reach a mixing of 52%, a similar value to the one obtained in the CFD model, 54%. Mixing is then solely due to molecular diffusion in this structure, reinforcing the ability of zigzag design to enhance the mixing.

Next, the zigzag channel was experimentally validated with a fluorescent tagged IgG molecule, FITC-IgG, mixed with a buffer solution. The MI found for the FITC-IgG is described in Figure 5A. A MI of 86% is achieved, slightly lower than the expected value of 98%. For the

FITC-IgG molecule, a degree of labeling (DoL) of 10 was calculated according to The and Feltkamp.[29] Thus, ten molecules of FITC are labeling a single molecule of IgG, which can significantly alter the physical proprieties of the antibody.[30] This high DoL will thus lead to a different mAb molecule, with a dissimilar diffusion coefficient to the ones assessed during the simulation work, explaining the small difference encountered for the MI. Additionally, the T-mixer was also validated with the FITC-IgG molecule and a MI of 49% was determined. Therefore, even though the proprieties of the molecule can influence the characteristics of the mAb stream to be mixed, a high MI is still reached for the designed channel, proving that in fact the zigzag geometry enhances mixing. Since molecular diffusion, which is dependent on the residence time of the molecule in the channel, plays a crucial role in mixing, by reducing the flow rate, the IgG molecule will then have enough mixing time to achieve proper mixing. For example, by using a flow rate of 0.5 μL min^{-1}, a MI of around 95% (Figure 5A() and D) is achieved. Nevertheless, the zigzag geometry allows for the generation of some advection, by folding the laminar flow and allowing the streamlines to cross each other. The different MIs experimentally obtained for the T-mixer and for the zigzag channel clearly demonstrate the mixing efficiency provided by the latter. Therefore, the mass transport of the mAb molecule is not solely due to diffusion but also due to the path disturbance provided by the proposed geometry.

4 | CONCLUDING REMARKS

The design and development of a miniaturized mixer for the creation of a fluorescent dye-based PAT tool for aggregate detection is here described. Resorting to a passive mixing induction, by using different geometries and subsequent variations, the mixing of two streams in the microscale is achieved. A CFD model in COMSOL Multiphysics was developed to assess the mixing efficiency of four proposed designs: a straight, a zigzag, a curved serpentine and a square serpentine channel. From the screening of the various geometries, the zigzag channel presented the highest mixing efficiency. The mixing occurs due to a balance of the presence of path crossing and void areas induced by the zigzag angle. Therefore, the zigzag channel with a 45° angle showed a high MI, of around 98%, in the 3D simulation. The design criteria imposed were all fulfilled: 1) the micromixer is expected not to alter the amount of aggregates due to the low shear rate calculated; 2) a high mixing efficiency of above 90%; is achieved; 3) a real-time measurement is accomplished in under 30 s. Furthermore, due to the low pressure drop and reduced footprint, the micromixer is easy to fabricate in PDMS and to operate. A wide range of mAb solutions conditions were also tested in the CFD model by varying the viscosity and diffusion coefficient to assess the robustness of the developed micromixer. A MI of at least 97% was obtained for all combinations of conditions tested, demonstrating the capability to detect aggregates in a variety of manufacturing processes.

The final designed micromixer was then experimentally validated, first, resorting to color dyes, and then to a fluorescent tagged IgG molecule (FITC-IgG). A MI of 98% was obtained in the end of the channel with the color dyes, validating the mixing efficiency proposed by the CFD model. For the FITC-IgG validation, a MI of 86% was reached at the end of the channel. This lower value can be explained by the high DoL of this molecule, which can significantly impact the mAb physical proprieties.[30] Nevertheless, even though small differences are encountered between the CFD model and experimental validation (Figure 5A), the proposed zigzag channel is still able to induce mixing in a fast and efficiently manner. The next step will be to verify the capability of the proposed structure to actually detect aggregates. Due to the high affinity of the fluorescent dyes to mAb aggregates, it was assumed that if the solutions were in contact, the fluorescent dyes would instantly interact with the aggregates and a fluorescence signal would be emitted. However, this assumption still needs to be experimentally validated. Nevertheless, a simple design for providing efficient mixing of two streams under 30 s was hereby demonstrated.

AUTHOR CONTRIBUTIONS

Mariana N. São Pedro: Conceptualization; Investigation; Methodology; Software; Validation; Writing – original draft. Mafalda S. Santos: Conceptualization; Investigation; Software; Writing – review & editing. Michel H. M. Eppink: Conceptualization; Investigation; Supervision; Writing – review & editing. Marcel Ottens: Conceptualization; Funding acquisition; Investigation; Supervision; Writing – review & editing.

ACKNOWLEDGEMENTS

The authors wish to thank the European Union's Horizon 2020 research and innovation programme under the Marie Skłodowska-Curie grant agreement No 812909 CODOBIO, within the Marie Skłodowska-Curie European Training Networks framework.

CONFLICT OF INTEREST

The authors declare no financial or commercial conflict of interest.

DATA AVAILABILITY STATEMENT

The data that support the findings of this study are available from the corresponding author upon reasonable request.

ORCID

Mariana N. São Pedro https://orcid.org/0000-0002-1801-9629
Michel H. M. Eppink https://orcid.org/0000-0001-8297-9985

REFERENCES

1. São Pedro, M. N., Silva, T. C., Patil, R., & Ottens, M. (2021). White paper on high-throughput process development for integrated continuous biomanufacturing. *Biotechnology and Bioengineering*, *118*, 3275–3286.
2. Grilo, A. L., & Mantalaris, A. (2019). The increasingly human and profitable monoclonal antibody market. *Trends in Biotechnology*, *37*, 9–16.
3. São Pedro, M. N., Klijn, M. E., Eppink, M. H. M., & Ottens, M. (2021). Process analytical technique (PAT) miniaturization for monoclonal antibody aggregate detection in continuous downstream processing. *Journal of Chemical Technology and Biotechnology*, *97*, .
4. Walchli, R., Ressurreicao, M., Vogg, S., Feidl, F., Angelo, J., Xu, X., Ghose, S., Li, Z. J., Saoût, X. L., Souquet, J., Broly, H., & Morbidelli, M. (2020). Understanding mAb aggregation during low pH viral inactivation and

subsequent neutralization. *Biotechnology and Bioengineering*, *117*, 687–700.
5. Thomas, C. R., & Geer, D. (2011). Effects of shear on proteins in solution. *Biotechnol. Lett*, *33*, 443–456.
6. Mahler, H. C., Friess, W., Grauschopf, U., & Kiese, S. (2009). Protein aggregation: Pathways, induction factors and analysis. *Journal of Pharmaceutical Sciences*, *98*, 2909–2934.
7. Somasundaram, B., Pleitt, K., Shave, E., Baker, K., & Lua, L. H. L. (2018). Progression of continuous downstream processing of monoclonal antibodies: Current trends and challenges. *Biotechnology and Bioengineering*, *115*, 2893–2907.
8. Hawe, A., Sutter, M., & Jiskoot, W. (2008). Extrinsic fluorescent dyes as tools for protein characterization. *Pharmaceutical Research*, *25*, 1487–1499.
9. Paul, A. J., Schwab, K., Prokoph, N., Haas, E., Handrick, R., & Hesse, F. (2015). Fluorescence dye-based detection of mAb aggregates in CHO culture supernatants. *Anal. Bioanal. Chem*, *407*, 4849–4856.
10. He, F., Phan, D. H., Hogan, S., Bailey, R., Becker, G. W., Narhi, L. O., & Razinkov, V. I. (2010). Detection of IgG aggregation by a high throughput method based on extrinsic fluorescence. *Journal of Pharmaceutical Sciences*, *99*, 2598–2608.
11. Oshinbolu, S., Shah, R., Finka, G., Molloy, M., Uden, M., & Bracewell, D. G. (2018). Evaluation of fluorescent dyes to measure protein aggregation within mammalian cell culture supernatants. *Journal of Chemical Technology and Biotechnology*, *93*, 909–917.
12. Hawe, A., Friess, W., Sutter, M., & Jiskoot, W. (2008). Online fluorescent dye detection method for the characterization of immunoglobulin g aggregation by size exclusion chromatography and asymmetrical flow field flow fractionation. *Analytical Biochemistry*, *378*, 115–122.
13. Sia, S. K., & Whitesides, G. M. (2003). Microfluidic devices fabricated in poly(dimethylsiloxane) for biological studies. *Electrophoresis*, *24*, 3563–3576.
14. Javaid, M. U., Cheema, T. A., & Park, C. W. (2017). Analysis of passive mixing in a serpentine microchannel with sinusoidal side walls. *Micromachines (Basel)*, *9*, 8.
15. Cai, G., Xue, L., Zhang, H., & Lin, J. (2017). A review on micromixers, *Micromachines (Basel)*, *8*, 274.
16. Lee, C.-Y., Wang, W.-T., Liu, C.-C., & Fu, L.-M. (2016). Passive mixers in microfluidic systems: A review. *Chem. Eng. J.*, *288*, 146–160.
17. Ward, K., & Fan, Z. H. (2015). Mixing in microfluidic devices and enhancement methods. *Journal of Micromechanics and Microengineering*, *25*, 094001.
18. Tsai, C. D., & Lin, X. Y. (2019). Experimental study on microfluidic mixing with different zigzag angles. *Micromachines (Basel)*, *10*, 583.
19. Rhoades, T., Kothapalli, C. R., & Fodor, P. S. (2020). Mixing optimization in grooved serpentine microchannels. *Micromachines (Basel)*, *11*, 61.
20. Alam, A., Afzal, A., & Kim, K.-Y. (2014). Mixing performance of a planar micromixer with circular obstructions in a curved microchannel. *Chemical Engineering Research and Design*, *92*, 423–434.
21. Hashmi, A., & Xu, J. (2014). On the quantification of mixing in microfluidics. *Journal of Laboratory Automation*, *19*, 488–491.
22. Perry, R. H., Green, D. W., & Maloney, J. O. (1997). *Perry's chemical engineers handbook*. McGraw-Hill.
23. Pathak, J. A., Sologuren, R. R., & Narwal, R. (2013). Do clustering monoclonal antibody solutions really have a concentration dependence of viscosity? *Biophysical Journal*, *104*, 913–923.
24. Woldeyes, M. A., Qi, W., Razinkov, V. I., Furst, E. M., & Roberts, C. J. (2019). How well do Low- and High-Concentration protein interactions predict solution viscosities of monoclonal antibodies? *Journal of Pharmaceutical Sciences*, *108*, 142–154.
25. Bee, J. S., Stevenson, J. L., Mehta, B., Svitel, J., Pollastrini, J., Platz, R., Freund, E., Carpenter, J. F., & Randolph, T. W. (2009). Response of a concentrated monoclonal antibody formulation to high shear. *Biotechnology and Bioengineering*, *103*, 936–943.
26. Khosravi Parsa, M., Hormozi, F., & Jafari, D. (2014). Mixing enhancement in a passive micromixer with convergent–divergent sinusoidal microchannels and different ratio of amplitude to wave length. *Comput. Fluids*, *105*, 82–90.
27. Pindrus, M. A., Shire, S. J., Yadav, S., & Kalonia, D. S. (2018). The effect of low ionic strength on diffusion and viscosity of monoclonal antibodies. *Mol Pharm*, *15*, 3133–3142.
28. Sudrik, C., Cloutier, T., Pham, P., Samra, H. S., & Trout, B. L. (2017). Preferential interactions of trehalose, L-arginine.HCl and sodium chloride with therapeutically relevant igg1 monoclonal antibodies. *mAbs*, *9*, 1155–1168.
29. The, T. H., & Feltkamp, T. E. W. (1970). Conjugation of fluorescein isothiocyanate to antibodies. *Immunology*, *18*, 865–873.
30. São Pedro, M. N., Azevedo, A. M., Aires-Barros, M. R., & Soares, R. R. G. (2019). Minimizing the influence of fluorescent tags on IgG partition in PEG-Salt aqueous two-phase systems for rapid screening applications. *Biotechnology Journal*, *14*, e1800640.

How to cite this article: São Pedro, M. N., Santos, M. S., Eppink, M. H. M., & Ottens, M. (2022). Design of a microfluidic mixer channel: first steps into creating a fluorescent dye-based biosensor for mAb aggregate detection. *Biotechnology Journal*, e2200332. https://doi.org/10.1002/biot.202200332